Simplified Risley Prism-Inspired 2D Beam Steering with a Tilted-Beam Resonant Cavity Antenna and Single Metasurface

Khushboo Singh, Dushmantha Thalakotuna and Karu Esselle
School of Electrical and Data Engineering
University of Technology Sydney
Sydney, Australia
khushboo.singh@uts.edu.au. karu.esselle@uts.edu.au

***Abstract*—This article presents a low-profile, mechanically beam-steerable antenna system inspired by a simplified Risley prism configuration. Unlike conventional Risley prism-based antennas that employ two beam-deflecting metasurfaces, the proposed two-dimensional beam-steering system combines a tilted-beam resonant cavity antenna with a single flat add-on metasurface, enabling agile beam steering with reduced mechanical complexity. The antenna features a compact aperture of $3.6\lambda_0 \times 3.6\lambda_0$ and an overall height of less than λ_0, making it ideal for low-profile applications. Full-wave simulations at 11.7 GHz demonstrate up to $\pm 50^\circ$ elevation scanning and full 360° azimuth coverage via mechanical rotation of the phase-gradient metasurface. The gain variation remains within 2.8 dB across the steering range, with a peak realized gain of 15 dBi at broadside.**

***Index Terms*—Risely prism, phase gradient, metasurface, beam steering, resonant cavity antenna, near-field, meta-steering**

I. Introduction

High-gain, compact antennas with beam-scanning capabilities are the cornerstone of emerging communication technologies that depend on space-based networks, particularly those utilizing Low Earth Orbit (LEO) and Medium Earth Orbit (MEO) satellites. Among various beam-steering methods, mechanical beam steering offers significant advantages. Unlike electronic beam steering, which involves complex circuitry and high power losses, particularly in the feed network and RF components like phase shifters and PIN diodes, mechanical methods often provide simpler, more cost-effective solutions without compromising performance, making them suitable for a wide range of applications [1]. As a result, mechanically beam-steerable antennas have seen significant advancements over the years. These developments have evolved from bulky parabolic reflectors to more efficient systems utilizing tilting flat-panel antennas. Further progress has led to tilt-free beam-steerable technologies, such as reflectarrays and transmitarrays, with the emergence of highly sophisticated and compact state-of-the-art solutions like near-field meta-steering antennas [1], [2].

Resonant cavity antennas (RCAs), consisting of a feed source, radiator, and a resonant cavity created between a ground plate and a partially reflecting superstrate (PRS), are well-known for their ability to achieve high gain with a compact profile. They are typically used in communication systems, radar, and other satellite-related technologies due to their high efficiency and performance. Over the years, several modifications have been implemented to the PRS of conventional RCAs to improve their overall radiation performance [3]–[6]. Metasurface-based partially reflecting surfaces in resonant cavity antennas leverage the unique properties of metasurfaces to create a cavity with controlled reflection and transmission, thereby enhancing antenna performance in terms of gain, bandwidth, and directivity [4]–[6]. Gradient metasurface-based PRS has been implemented in the past to tilt the beam to a fixed angle from the broadside direction [6]–[9]. Actively tunable PRSs have also been implemented to enable 2D beam steering in RCAs. However, this article focuses on investigating a passive gradient metasurface-based PRS for realizing beam steering within the RCA. Therefore, actively tunable PRSs are not discussed further here for the sake of brevity.

To the best of our knowledge, most passive PRS-based RCAs do not support continuous beam steering or full 2D beam scanning across the angular space, unless two phase-gradient metasurfaces are rotated independently over the near-field aperture of the RCA. This approach, called near-field meta-steering, is based on the principles of the Risley prism [10], [11] and has gained significant attention due to its simplicity and efficient beam-steering performance. Researchers have explored various configurations of Risley prism-based beam steering at microwave frequencies to reduce the overall antenna profile. These configurations range from a pair of bulky dielectric wedges [12], [13] to a pair of flat-panel phase-gradient metasurfaces. The flat-panel metasurfaces used in these beam-steering antennas have undergone several design modifications, including PCB-type composite metasurfaces [10], [11], [14], all-metal metasurfaces [15], perforated all-dielectric metasurfaces [16], and hybrid metasurfaces [17]. The use of low-profile directive feed antennas, such as radial line slot arrays, resonant cavity antennas, and metasurface antennas can further reduces the overall height of the beam-steering antenna system. However, all the aforementioned

antennas rely on two additional metasurfaces added to the base antennas to achieve complete beam scanning.

Recently, a new beam-scanning architecture based on a simplified Risley prism structure was proposed in [4]. The antenna achieves 2D beam steering using only a single flat phase-shifting metasurface and a holographic leaky-wave antenna, with the two components mechanically rotated independently against each other. Building on this concept, another study [18] introduced a 2D beam-scanning antenna system employing a quasi-optically fed metasurface antenna and a single metasurface composed of two additively manufactured, complementary parts: an array of quad-ridge waveguides in titanium and a dielectric filling made of acrylonitrile butadiene styrene (ABS). Similarly, in [19], a gradient-phase feed source combined with a gradient-phase transmitarray is used to achieve 2D beam steering, implementing the same simplified Risley prism principle. Inspired by the new simplified Risley prism architecture, we propose a new 2D beam-scanning antenna design composed of a printed gradient PRS-based RCA and a single printed PCB-type phase-gradient metasurface. To the best of the author's knowledge, this work represents the first implementation of complete 2D beam-scanning RCA with a single metasurface.

The rest of the article is structured as follows: Section II details the design methodology for the 2D beam-steering antenna based on simplified Risly prism principle. First, a tilted beam RCA is designed to create a 1-D beam-steering system, followed by the design and implementation of a phase-gradient metasurfaces for 2D beam scanning. The simulation results are also presented. Section III provides the conclusion.

II. Design Methodology

A 2D beam-steerable antenna based on the concept of a simplified Risley prism is proposed [18]. The antenna system consists of a tilted-beam resonant cavity antenna and a phase-gradient metasurface placed in the near field, very close to its aperture. The design details for each antenna component are thoroughly described in the following sub-sections.

A. Base Antenna Configuration

A low-profile resonant cavity antenna is designed at the center frequency of 12 GHz using a metallic slot radiator excited by a WR-75 coax-to-waveguide adapter and a printed partially reflective superstrate, as shown in Fig. 1. The initial design of the RCA uses a printed PRS with uniform square metallic loops on the underside. This configuration enhances overall radiation performance in terms of directivity, realized gain, side-lobe level, and efficiency, compared to a bare dielectric PRS without metallic inclusions. Following the procedure outlined in the literature [6], the PRS is modified by making the square metallic loops non-uniform, with their width gradually varying across the aperture to create a phase gradient in order to implement beam tilt. The width of the metallic loops, denoted as w_i is varied such that the difference in width (Δw) between adjacent loops is constant. The design parameters for the two RCAs is listed in Table I. We investigated the

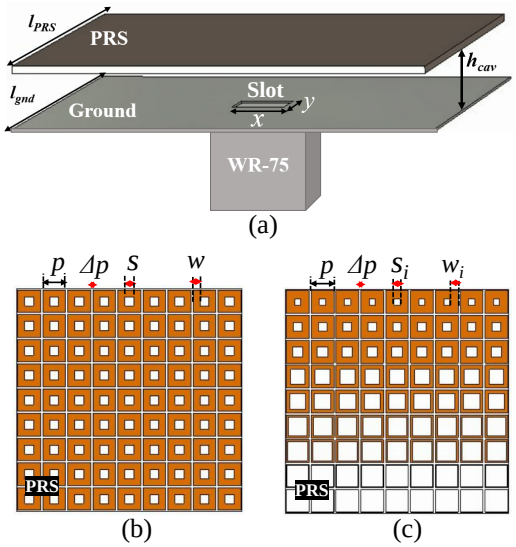

Fig. 1. Resonant cavity antenna configuration, showing (a) an isometric view of the antenna and the underside of the partially reflecting superstrate, with (b) uniform square metallic loops and (c) non-uniform, gradually varying metallic loops that create a transmission phase gradient.

TABLE I
Design Dimensions for the Resonant Cavity Antennas.

Design Parameters	RCA with uniform metallic loops in PRS	RCA with non-uniform metallic loops in PRS
p	9 mm)	9 mm
Δp	0.87 mm	0.87
h_{cav}	13.41 mm	13.41 mm
l_{gnd}	90 mm	90 mm
x	12.47 mm	12 mm
y	9.5 mm	9.5 mm
Δw	0	0.25, 0.50, 0.75
w_i	2.7 mm	$w_6 + (i-6)\Delta w$
s_i	$9 - 2w_i$	$9 - 2w_i$

$*w_6$ is fixed at 1.835 mm and w_1 to w_9 is varied such that $w_i = w_6 + (i-6)\Delta w$ and $i = 1, 3, ...9$ and $s_i = 9 - 2w_i$. For all $w_i \leq 0$, $s_i = 9$.

performance of the RCA for three different values of Δw: 0.25, 0.5, and 0.75. Full-wave electromagnetic simulations were carried out in CST Microwave Studio (MWS) using the time-domain solver with open boundary conditions. The resulting peak gain and beam-tilt angles achieved through the RCA for Δw values of 0.25, 0.5, and 0.75 were as follows: 17.7 dBi with a tilt of 24° at 12.5 GHz, 16.4 dBi with a tilt of 34° at 11.4 GHz, and 14.6 dBi with a tilt of 37°, respectively. Thus, it is established that the beam tilt angle is primarily determined by the gradient introduced in the PRS structure. The PRS configuration with $\Delta w = 0.5$ is further optimized using CST's built-in local optimization algorithm, the Trust Region Framework, to improve directivity and suppress side lobes across the 11.5–12.5 GHz frequency band, while ensuring good impedance matching of the antenna. The slot dimensions, s_i, cavity height (h_{cav}), Δp, x and y were selected as the optimization parameters, with other design variables listed in Table. I kept fixed. The initial and optimized values of s_i are provided in Table II.

TABLE II
DESIGN DIMENSIONS FOR OPTIMIZED TILTED-BEAM RESONANT CAVITY ANTENNA.

Optimization Parameter (s_i)	Initial Dimensions (mm)	Optimized Dimensions (mm)
s_1	9	8.97
s_2	9	8.55
s_3	8.33	7.67
s_4	7.33	7.35
s_5	6.33	6.40
s_6	5.33	5.84
s_7	4.33	4.06
s_8	3.33	3.36
s_9	2.33	2.43
h_{cav}	13.41	12.17
x	12	11.24
y	9.5	9.46
Δp	0.87	0.78

$*$for initial design $\Delta w = 0.5$.

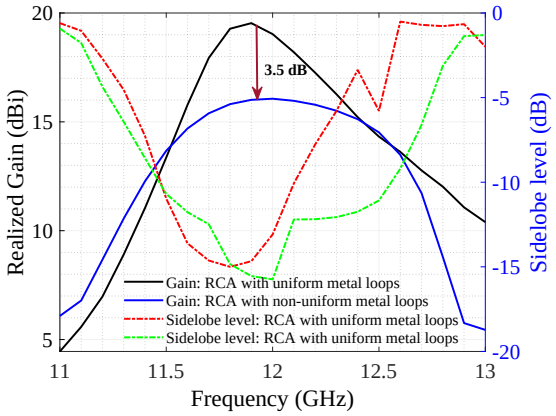

(a)

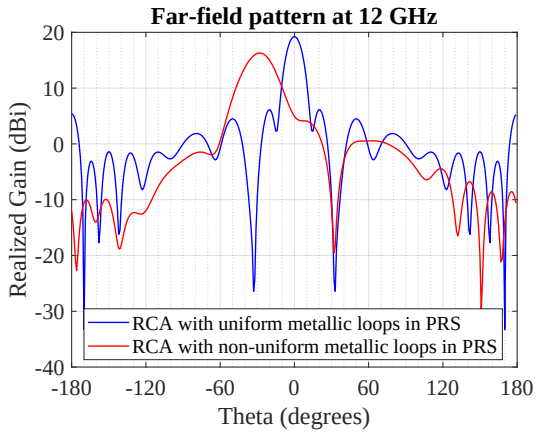

(b)

Fig. 2. Comparing the radiation characteristics of RCA with uniform and non-uniform metallic loops in the PRS, when PRS is oriented at $\Psi_1 = 90°$. (a) Realized gain and side-lobe level variation over frequency. (b) Elevation-plane radiation pattern cuts at $\Phi = 90°$.

Fig. 2(a) illustrates the simulated radiation performance across the targeted frequency band and Fig. 2(b) shows the simulated radiation patterns at the center frequency for the two RCA configurations: one employing uniform metallic loops in the PRS, and the other utilizing an optimized beam-tilting design with non-uniform metallic loops. It is observed that the implementation of non-uniform loops in the PRS leads to a noticeable reduction in gain, with the maximum gain being up to 3.5 dB lower than that achieved by the configuration with uniform loops. The reduction in overall gain is attributed to the partial illumination of the PRS aperture when non-uniform metallic loops are employed. As discussed in [6], for a fixed aperture length along the direction of uniform phase, the gain is primarily influenced by the extent of the in-phase region spreading in the direction having a phase gradient. Consequently, increasing the number of metallic loops along the gradient leads to a larger in-phase area, thereby enhancing the overall gain. However, it should be noted that the overall gain is still higher compared to the one achieved by a bare dielectric PRS. The optimized RCA with non-uniform metallic loops in PRS generates a tilted beam $-28°$ away from the broadside. The side-lobe levels are below -10 dB from 11.4 GHz to 12.6 GHz. At the center frequency of 12 GHz, the antenna achieves a maximum gain of 16.3 dBi with the main beam directed at $-28°$ in elevation (Fig. 2(a)). Further simulations show that the beam is tilted to $-27°$ with a corresponding gain of 15.6 dBi at 11.7 GHz, while at 12.2 GHz, the beam direction shifts to $-29°$, with a peak gain of 16.2 dBi. These results confirm the stable beam-tilting behavior of the RCA and consistent high-gain performance over the operating frequency range.

B. 1-D Beam-Steering

To enable one-dimensional beam steering with the tilted-beam resonant cavity antenna design, the top PRS layer was mechanically rotated about its central axis. This rotation enables beam steering in the azimuth plane while maintaining a fixed elevation angle (Θ), allowing continuous azimuthal beam positioning (Φ) over a full $0°$ to $360°$ range. This behavior is clearly illustrated in Fig. 3, which shows the rotation of the beam in the 3-D radiation patterns within the azimuth plane, resulting from the physical rotation the PRS denoted by angle ψ_1.

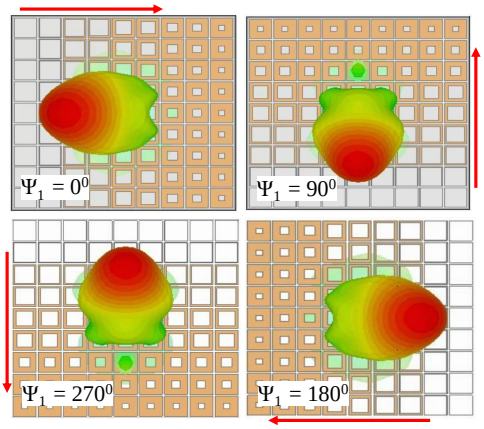

Fig. 3. 3-D radiation patterns of the resonant cavity antenna for different orientations of the PRS.

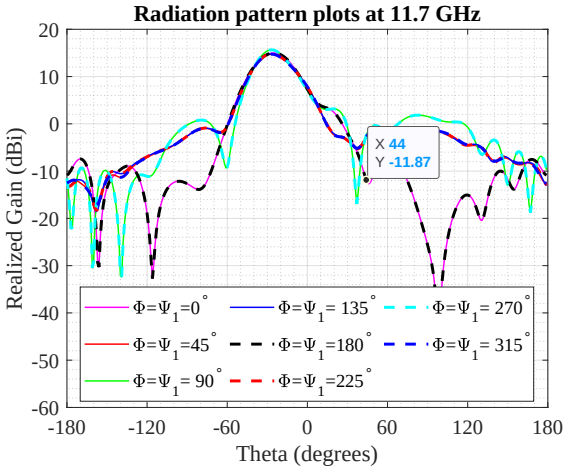

(a)

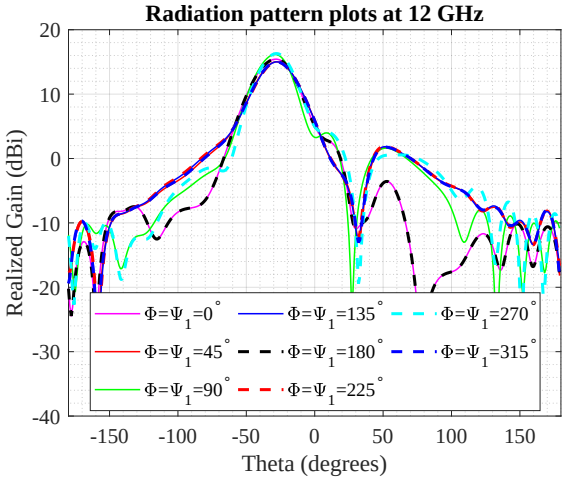

(b)

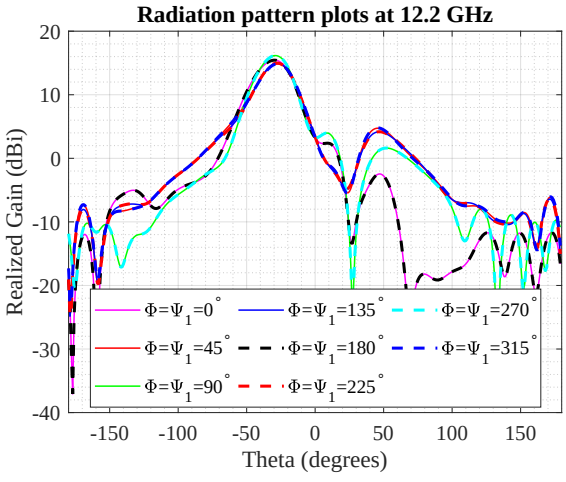

(c)

Fig. 4. Comparison of Radiation Characteristics of the RCA with Uniform and Non-Uniform Metallic Loops in the PRS (a) Realized gain and side-lobe-level; and (b) Elevation-plane radiation pattern cuts at $\Phi = 90^\circ$ for the PRS oriented at $\Psi_1 = 90^\circ$.

In Fig. 4 a fixed beam tilt of approximately $\Theta = 30^\circ$ in the elevation plane is achieved while enabling full beam steering in the azimuth plane. It is observed that the azimuth angle of the main beam, corresponds directly to the orientation of the PRS with respect to the x-axis such that , $\Phi = \psi_1$. Across all three frequencies—11.7 GHz (Fig. 4(a)), 12 GHz (Fig. 4(b)), and 12.2 GHz (Fig. 4(c))—the main beam consistently exhibits an elevation angle between -25° to -30° while the azimuth angle can be steered continuously over the full 0° to 360° range.

C. 2D Beam-Steering

The rotation of the PRS enables beam across all azimuth angles from 0° to 360°. However, achieving full two-dimensional beam steering in both the elevation and azimuth planes necessitates the integration of a phase-gradient metasurface as an add-on to the tilted-beam RCA. To enable comprehensive beam scanning within a conical region, a PGM is designed to deflect a normally incident beam to an elevation angle of approximately 30° ($\delta = 30^\circ$). The configuration of the unit cell implemented to design the PGM is shown in Fig. 5. It consists of three dielectric layers of Taconic TLY-5 ($\varepsilon_r = 2.2$), each 1.52 mm thick, and four layers of square-shaped metallic printed patterns. The length of each square unit cell is $d = 2\lambda_\circ/5$ (10 mm @ 12 GHz). The top and bottom metallic layers of the unit cell are identical, each having a side length L_1, while the two intermediate square-shaped layers share a common side length L_2. The unit cell was simulated in CST MWS with unit cell boundary condition and Floquet port excitation. A parameter sweep was performed, varying the design variables L_1 and L_2 between 0.05 mm to 9 mm and the resulting transmission phase and magnitude responses were recorded and stored in a database for subsequent use in metasurface design.

A phase gradient metasurface (PGM) is constructed using the same unit cell shown in Fig. 5 to deflect a normally incident plane wave and achieve a beam tilt of 30° in the far field. To realize this functionality, nine distinct unit cells are arranged along the x-direction to form a one-dimensional (1D) PGM. Each selected unit cell exhibits a high transmission ($S_{21} > -1.8$ dB) and the adjacent unit cells maintain a 72° phase delay between them. An array of 9×9 unit cells is

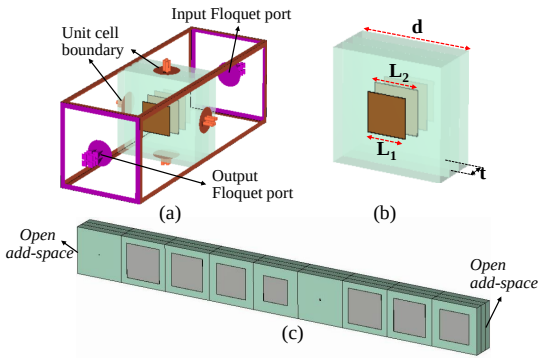

Fig. 5. Perspective view of the phase transforming unit cell showing the (a) boundary conditions used for simulation, (b) the design parameters and (c) the 1-D phase-gradient metasurface.

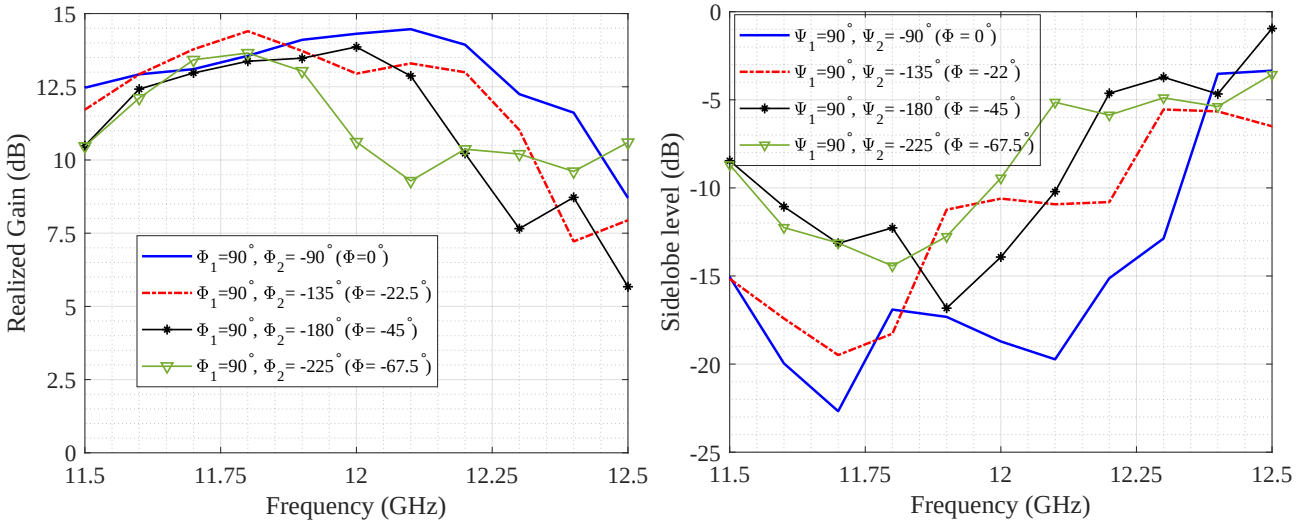

Fig. 6. Radiation characteristics of the 2D beam-scanning antenna for various orientations of the PGM, with the PRS fixed at $\Psi_1 = 90°$: (a) Realized gain variation over frequency, and (b) Side-lobe level variation over frequency.

required to cover the aperture of the antenna. Therefore, the 1-D PGM is then replicated nine times along the y-direction to create a complete 2D metasurface. The beam-tilt angle δ of the metasurface is determined using equation1, as described in [11].

$$\Delta\phi = \frac{2\pi}{\lambda_\circ} d \sin\delta \tag{1}$$

where $d = 2\lambda_0/5$ is the size of the unit cell in terms of free-space wavelength and $\Delta\phi = 2\pi/5$ is the phase delay between adjacent unit cells. The design methodology for phase-gradient metasurfaces is well-documented in the literature [11], [20] and is therefore not reiterated in this work for the sake of brevity. The PGM is positioned 2 mm above the PRS of the resonant cavity antenna and is mechanically rotated about its central axis, while the PRS is held fixed at an orientation of $\Psi_1 = 90°$. The variation of realized gain and side-lobe level across frequency, observed at the Φ-cut corresponding to the beam peak direction, is presented in Fig. 6. The corresponding orientation of PRS (Ψ_1) and PGM (Ψ_2) are indicated in the plot legends for clarity. The highest peak gain of 14.8 dB is observed when the beam is directed broadside at 12.1 GHz. However, for frequencies above 11.9 GHz, both the realized gain and side-lobe levels degrade significantly in the case of extreme beam tilt. Meanwhile, within the 11.5–11.9 GHz range, the antenna system demonstrates effective beam-steering performance with minimal variation in realized gain and side-lobe levels consistently maintained below –10 dB.

Beam steering in both the elevation and azimuth planes, achieved through this rotational manipulation of the PGM, is illustrated by the 3-D radiation patterns shown for various PGM orientations in Fig. 7. Fig. 8 shows the far-field radiation pattern cuts at 11.7 GHz, taken at elevation planes where the beam peak exists. In this case, the beam peaks occur along

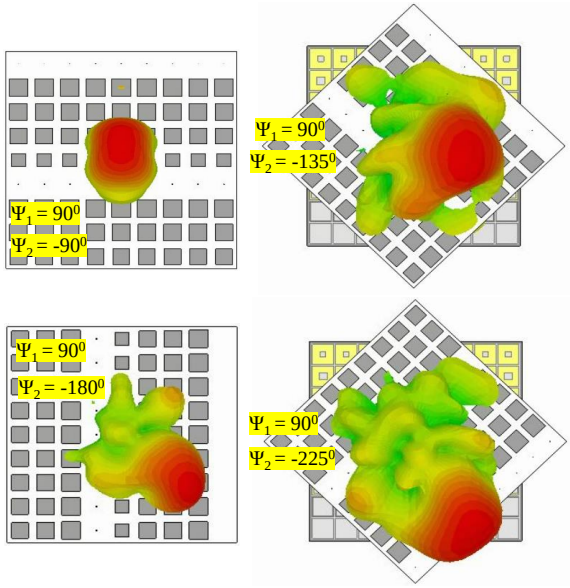

Fig. 7. 3D radiation patterns of the 2D beam-steering antenna system illustrating the beam direction shift corresponding to different orientations of PGM over the fixed PRS.

$\Phi = (\Psi_1 + \Psi_2)/2$. For other orientations of PRS and PGM, the beam location (Θ, Φ) can be calculated from equation available in literature [11]. The orientations of both the major and minor lobes are illustrated in the figure. The maximum side-lobe level is observed when the beam is steered to its maximum tilt in the elevation plane, at $\theta = 50°$, measuring approximately –12 dB at 11.7 GHz. The beam-steering system is capable of tilting the main beam up to $\pm 50°$ in elevation. Across all steering angles in the plane containing the beam peak, side-lobe levels remain below –12 dB, indicating effective suppression of undesired radiation.

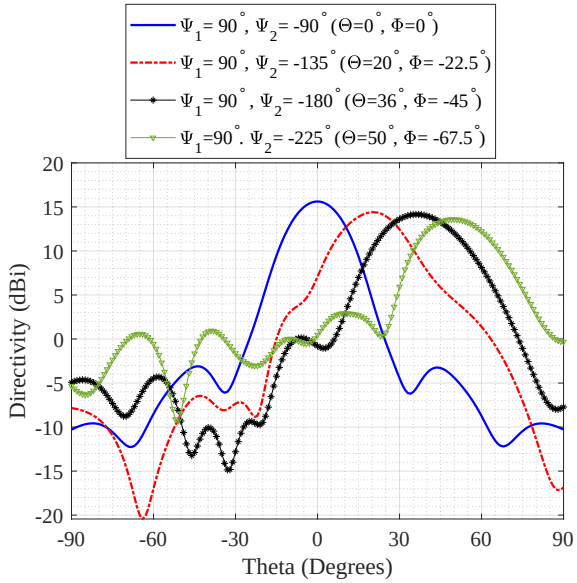

Fig. 8. Elevation-plane radiation pattern cuts taken at the azimuth angle Φ corresponding to the beam peak direction, for the PRS fixed at $\Psi_1 = 90°$, with varying orientations of the PGM.

III. Conclusion

A compact, low-profile, 2D beam-steerable antenna system operating in the Ku-band is presented, leveraging a simplified implementation of the Risley prism concept. In contrast to conventional Risley prism-based beam-scanning antennas—which typically rely on at least two additional metasurfaces—the proposed design integrates a tilted-beam resonant cavity antenna with a single, passive phase-gradient metasurface to achieve comprehensive dynamic beam steering. The metasurface can be positioned in close proximity to the PRS, at a distance of approximately 2 mm, without degrading the antenna's performance. This configuration results in a substantial reduction in both the structural complexity and overall thickness of the beam-steerable antenna system, offering a streamlined and efficient solution for high-frequency beam steering applications. The the antenna is capable of performing 2D beam scanning over $\pm 50°$ field of view within a gain variation of less than 2.8 dB. The measured peak directivity is 15.3 dB when the beam is in broadside. The concept is particularly promising for applications where moderate scanning speed can be traded off for reduced system cost, thickness, and mechanical simplicity.

Acknowledgments

This research was partially funded by UTS and the Australian Government through the Office of National Intelligence - National Intelligence and Security Discovery Research Grant program, Project ID NI240100157

References

[1] K. Esselle, K. Singh, D. Thalakotuna, M. N. Y. Koli, and F. Ahmed, "Beam-steering antenna technologies for space-related applications," in *2023 17th European Conference on Antennas and Propagation (EuCAP)*. IEEE, 2023, pp. 1–5.

[2] I. Uchendu and J. R. Kelly, "Survey of beam steering techniques available for millimeter wave applications," *Progress In Electromagnetics Research*, vol. 68, pp. 35–54, 2016.

[3] K. Singh, M. Attygalle, D. Thalakotuna, and K. Esselle, "Multi-feed resonant cavity antenna with in-antenna power combination for mm-wave communication," in *2024 18th European Conference on Antennas and Propagation (EuCAP)*. IEEE, 2024, pp. 1–5.

[4] Z. Zhang, Y. C. Zhong, H. Luyen, J. H. Booske, and N. Behdad, "A low-profile, risley-prism-based, beam-steerable antenna employing a single flat prism," *IEEE Transactions on Antennas and Propagation*, vol. 70, no. 8, pp. 6646–6658, 2022.

[5] H. Umair, T. B. A. Latef, Y. Yamada, T. Hassan, W. N. L. B. W. Mahadi, M. Othman, K. Kamardin, and M. I. Hussein, "Fabry-perot antenna employing artificial magnetic conductors and phase gradient metasurface for wideband monostatic rcs reduction and high gain tilted beam radiation," *IEEE Access*, vol. 9, pp. 66 607–66 625, 2021.

[6] H. Nakano, S. Mitsui, and J. Yamauchi, "Tilted-beam high gain antenna system composed of a patch antenna and periodically arrayed loops," *IEEE Transactions on Antennas and Propagation*, vol. 62, no. 6, pp. 2917–2925, 2014.

[7] S. Zheng, Y. Li, S. Gao, L. Zhao, W. Hu, Y. Cai, Q. Luo, and C. Gu, "A low-profile 2d tilted-beam resonant cavity antenna," in *12th European Conference on Antennas and Propagation (EuCAP 2018)*. IET, 2018, pp. 1–4.

[8] B. Ratni, J. Yi, X. Ding, A. de Lustrac, K. Zhang, G.-P. Piau, and S. N. Burokur, "Gradient phase partially reflecting surfaces for beam steering in microwave antennas," *Optics express*, vol. 26, no. 6, pp. 6724–6738, 2018.

[9] A. Ghasemi, S. N. Burokur, A. Dhouibi, and A. De Lustrac, "Phase-gradient metasurfaces for beam steerable antennas," in *2014 International Workshop on Antenna Technology: Small Antennas, Novel EM Structures and Materials, and Applications (iWAT)*. IEEE, 2014, pp. 191–194.

[10] M. I. Nabeel, M. U. Afzal, K. Singh, D. N. Thalakotuna, and K. P. Esselle, "Dual-band printed near-field metasurface with independent phase transformation for enhanced antenna gain," *IEEE Antennas and Wireless Propagation Letters*, 2024.

[11] K. Singh, M. U. Afzal, M. Kovaleva, and K. P. Esselle, "Controlling the most significant grating lobes in two-dimensional beam-steering systems with phase-gradient metasurfaces," *IEEE Transactions on Antennas and Propagation*, vol. 68, no. 3, pp. 1389–1401, 2019.

[12] H. Griffiths and M. Khan, "Antenna beam steering technique using dielectric wedges," in *IEE Proceedings H (Microwaves, Antennas and Propagation)*, vol. 136, no. 2. IET, 1989, pp. 126–131.

[13] A. A. Baba, R. M. Hashmi, K. P. Esselle, M. Attygalle, and D. Borg, "A millimeter-wave antenna system for wideband 2-d beam steering," *IEEE Transactions on Antennas and Propagation*, vol. 68, no. 5, pp. 3453–3464, 2020.

[14] N. Gagnon and A. Petosa, "Using rotatable planar phase shifting surfaces to steer a high-gain beam," *IEEE transactions on antennas and propagation*, vol. 61, no. 6, pp. 3086–3092, 2013.

[15] M. I. Nabeel, M. U. Afzal, K. Singh, D. N. Thalakotuna, and K. P. Esselle, "Waveguide-based all-metal near-field metasurfaces for linearly and circularly polarized beam steering antennas," *IEEE Access*, 2025.

[16] A. A. Baba, R. M. Hashmi, M. Attygalle, K. P. Esselle, and D. Borg, "Ultrawideband beam steering at mm-wave frequency with planar dielectric phase transformers," *IEEE Transactions on Antennas and Propagation*, vol. 70, no. 3, pp. 1719–1728, 2021.

[17] M. U. Afzal, K. P. Esselle, and M. N. Y. Koli, "A beam-steering solution with highly transmitting hybrid metasurfaces and circularly polarized high-gain radial-line slot array antennas," *IEEE Transactions on Antennas and Propagation*, vol. 70, no. 1, pp. 365–377, 2021.

[18] M. Bertrand, J. Ruiz-García, J.-F. Allaeys, D. G. Ovejero, T. Hoang, B. Loiseaux, R. Sauleau, R. Czarny, and M. Ettorre, "Risley scanner using a metasurface source and a single deflector for satcom applications," *IEEE Transactions on Antennas and Propagation*, 2024.

[19] J. Wang and Y. Rahmat-Samii, "A simplified configuration of beam-steerable risley prism antennas: Principles and validation," *IEEE Antennas and Wireless Propagation Letters*, vol. 21, no. 11, pp. 2288–2292, 2022.

[20] M. U. Afzal and K. P. Esselle, "Steering the beam of medium-to-high gain antennas using near-field phase transformation," *IEEE Transactions on Antennas and Propagation*, vol. 65, no. 4, pp. 1680–1690, 2017.